Journal of Alloys and Compounds 509 (2011) 5364–5367

Contents lists available at ScienceDirect

Journal of Alloys and Compounds

journal homepage: www.elsevier.com/locate/jallcom

Effect of lanthanum doping on linear and nonlinear-optical properties of Bi_3TiNbO_9 thin films

Hengzhi Chen[a], Bin Yang[a,*], Mingfu Zhang[b], Feiyan Wang[c], Kokwai Cheah[c], Wenwu Cao[a,d]

[a] Center for Condensed Matter Science and Technology, Department of Physics, Harbin Institute of Technology, Harbin 150001, China
[b] Center for Composite Materials, Harbin Institute of Technology, Harbin 150001, China
[c] Department of Physics, Hong Kong Baptist University, Hong Kong SAR, China
[d] Materials Research Institute, The Pennsylvania State University, University Park, PA 16802, USA

ARTICLE INFO

Article history:
Received 22 October 2010
Received in revised form 8 February 2011
Accepted 9 February 2011
Available online 15 February 2011

Keywords:
Nonlinear optical absorption
Lanthanum doped Bi_3TiNbO_9
Pulsed laser deposition
Optical constant

ABSTRACT

Lanthanum doped Bi_3TiNbO_9 thin films (LBTN-*x*, La^{3+} contents *x* = 5%, 15%, 25% and 35 mol.%) with layered perovskite structure were fabricated on fused silica by pulsed laser deposition method. Their linear and nonlinear optical properties were studied by transmittance measurement and Z-Scan method. All films exhibit good transmittance (>55%) in visible region. For lanthanum doping content are *x* = 5%, 15% and 25 mol.%, the nonlinear absorption coefficient of LBTN-*x* thin films increases with the La^{3+} content, then it drops down at *x* = 35 mol.% when the content of La^{3+} in $(Bi_2O_2)^{2+}$ layers is high enough to aggravate the orthorhombic distortion of the octahedra. We found that, 25 mol.% is the optimal La^{3+} content for LBTN-*x* thin films to have the largest nonlinear absorption coefficient making the LBTN-*x* film a promising candidate for absorbing-type optical device applications.

1. Introduction

Ferroelectric thin films have great potential for photonics applications due to their high optical nonlinearity, fast response and good compatibility with the fabrication process of waveguide and integrated-optic devices. Although ferroelectric (Pb,La)(Zr,Ti)O_3 (PLZT) thin films with perovskite structure are well-known candidates, which have attracted much attention in the past decade [1,2], the toxicity of lead restricts its applications in certain areas. Recent research exhibited that most bismuth layer-structured ferroelectric (BLSF) thin films, a kind of lead-free materials, also have excellent linear and nonlinear optical properties [3–5]. Among BLSF materials, Bi_3TiNbO_9 (BTN) has attracted more attention due to its high Curie temperature (T_c > 900 °C) [3,6–8]. There are a number of investigations on the crystal structure, synthesis and electrical properties of La^{3+} doped BLSF ceramics [9–12]. Zhu et al. reported that the concentration of oxygen vacancy decreases with La^{3+} doping in BLSF ceramics, which bring about the increasing of the remnant polarization. When the La^{3+} content is greater than a critical value, the distortions of octahedra become drastically, inducing a decrease of the remnant polarization [12]. Most of recent works focus on the issues of doping site of La^{3+} and try to understand the crystal structural changes caused by the La^{3+} substitution. However, the effect of La^{3+} ions doping on optical properties of the BTN thin films has not been systematically studied up to now.

This letter reports an experimental investigation of the optical properties of La^{3+} doped BTN thin films grown on silica substrates by pulsed laser deposition (PLD). The band gap, linear refractive index and linear absorption coefficient were obtained by optical transmittance measurement. The nonlinear optical absorption property of the films was investigated by the Z-scan technique with femtosecond laser pulses.

2. Experimental

Lanthanum doped Bi_3TiNbO_9 [LBTN-*x*, La^{3+} contents *x* = 5%(L1), 15%(L2), 25%(L3), 35 mol.%(L4)] pellets used as PLD targets were prepared by conventional solid-state reaction technique with starting materials Bi_2O_3, TiO_2, Nb_2O_5, and La_2O_3 in powder form. The powders were mixed by ball milling in ethanol for 12 h, then the dried mixture was calcined at 700 °C for 3 h. Excess 20 mol.% Bi_2O_3 was added to compensate for the Bi evaporation during the sintering process. In order to obtain dense LBTN-*x* ceramics, 5% polyvinyl alcohol solution prepared by immersion in a water bath at 90 °C was added to the mixed powders at the ratio of 1:95 (polyvinyl alcohol solution to the mixed powders). The screened uniform mixture of the powder was finally pressed into disks of 2 cm in diameter and sintered at 1000 °C for 2 h in a conventional box furnace. Dense yellowish pellets were acquired through this procedure.

The films were deposited by pulsed laser ablation on double-sided polished fused silica substrates with the surface area of 10 mm × 5 mm. A KrF excimer laser (LPX205i, Lambda Physik, 248 nm wavelength, 30 ns pulse width and 4 Hz repetition rate) was focused on the surface of a rotating target. The optimized deposition temperature, oxygen pressure and laser energy density were at 700 °C, 13 Pa and 2.0 J/cm^2, respectively. After deposition, all films were annealed *in situ* for 30 min with 0.5 atm O_2 pressure. In order to get a uniform thin film, the target and the substrate holder were rotated during deposition.

* Corresponding author.
E-mail address: binyang@hit.edu.cn (B. Yang).

0925-8388/$ – see front matter © 2011 Elsevier B.V. All rights reserved.
doi:10.1016/j.jallcom.2011.02.048

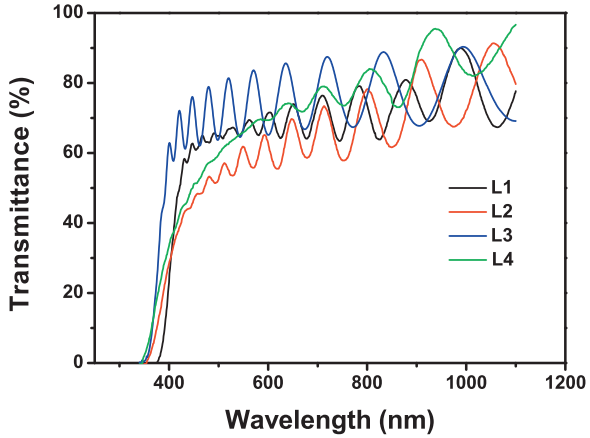

Fig. 1. Optical transmittance of LBTN-*x* thin film on fused silica substrate.

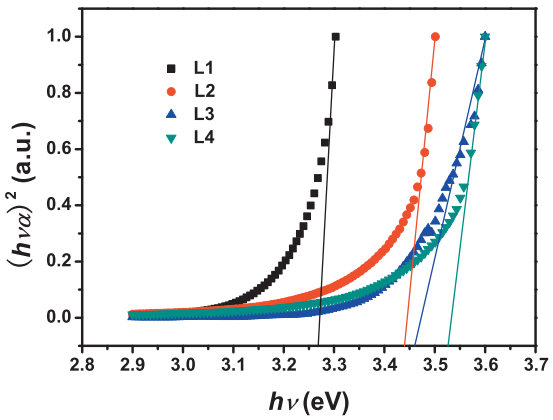

Fig. 2. Direct band gap of LBTN-*x* thin film as a function of photo energy.

The crystalline structure of the deposited films was characterized by X-ray diffraction (XRD). The optical transmittance spectra of the thin films were measured by a Hitachi U-3410 UV/VIS spectrophotometer. The nonlinear absorption coefficients of the LBTN-*x* films were determined by single-beam Z-scan technique. In our experiments, a Ti sapphire laser, with the wavelength of 800 nm, a repetition rate of 1 kHz, and a pulse width of 100 fs, was employed as the light source. The typical peak power density was 1 GW/cm^2. The sample transmission was monitored by a power meter.

3. Result and discussion

XRD patterns of LBTN-*x* thin films indicate that all deposited films are in single-phase structure. The transmittance spectra of the as-prepared LBTN-*x* thin films on the silica substrate with different La^{3+} content are shown in Fig. 1. All films exhibit very good transmittance (>55%) in visible region. It is clear that the transmittance drop in the high frequency side is due to interband absorption in the thin film. The oscillations in the transmittance come from the interference due to reflection from the top surface of the film and the interface between the film and substrate. The uniform periodic oscillating optical transmittance indicates that the film has a flat surface and a uniform thickness. The optical band gap energy E_g of the films are estimated from the graph of $(h\nu\alpha)^2$ vs $h\nu$ based on the relationship between the linear absorption coefficient α and the band gap energy E_g: $(h\nu\alpha)^2 = \text{const}(h\nu - E_g)$, where $h\nu$ is the incident light energy. Specifically, the value of E_g can be estimated by extrapolating the linear portion of the $(h\nu\alpha)^2$ vs $h\nu$ graph to $(h\nu\alpha)^2 = 0$ (Fig. 2). It is obvious from the experiment value in Table 1 that the band gap increases with La^{3+} content.

For a single-layer film with weak absorption on a transparent substrate, the linear refractive index n, absorption coefficient α and film thickness d can be obtained from the transmittance curve based on the envelope method [13,14]. The results are shown in Table 1. According to the Pikhtin–Yas'Kov model [15], band gap increases with the decrease of refractive index. Our experimental results are consistent with the Pikhtin–Yas'Kov model. As the of La^{3+} content increases, the refractive index of LBTN-*x* thin films decreases but the band gap of the thin films increases.

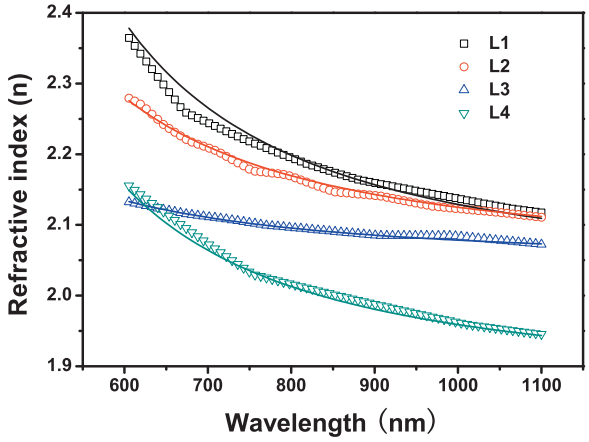

Fig. 3. Refractive index as a function of wavelength and the dispersion curve of LBTN-*x* thin films on fused silica substrates. The open symbols are experimental values while the solid lines are theoretical fittings.

Fig. 3 shows the relations between the refractive index and wavelength for the LBTN-*x* thin films. Data points are experimental results and the curves are from theoretical fitting. The refractive index of the LBTN-*x* thin film decreases drastically as the wavelength increases, showing a typical shape of a dispersion curve near an electronic interband transition. The dispersion data in the interband-transition region are modeled based on a single electronic oscillator. This theory assumes that the material is composed of a series of independent oscillators which are set into forced vibrations by incident radiations. According to the single electronic oscillator model proposed by Didomenico and Wemple [16], the dispersion of the refraction index can be described by the well-known Sellmeier relation:

$$n^2 = 1 + \frac{S_0\lambda_0^2}{1 - \left(\lambda_0/\lambda\right)^2}, \quad (1)$$

where λ_0 is the average oscillator position and S_0 is the average oscillator strength. By fitting the refractive-index data to Eq. (1),

Table 1
Thickness, band gap, refractive index, and linear absorption coefficient of LBTN-*x* thin film with different concentration of La^{3+}.

Sample	La^{3+} content (mol.%)	Thickness (μm)	Band gap (eV)	Refractive index at λ = 800 nm	Linear absorption coefficient at λ = 800 nm (×10^4 m^{-1})
L1	0.15	1.506	3.269	2.195	7.159
L2	0.45	1.452	3.440	2.168	11.350
L3	0.75	1.215	3.461	2.095	9.288
L4	1.05	1.372	3.525	2.016	3.035

Table 2
Average oscillator position, average oscillator strength, energy of the oscillator, and nonlinear absorption coefficient β of LBTN-x thin film with different concentration of La^{3+}.

Sample	Average oscillator position (nm)	Average oscillator strength (m^{-2})	Energy of the oscillator (eV)	β (fitting for 2PA, $\times10^{-7}$ m/W)	β (fitting for 3PA, $\times10^{-7}$ m/W)
L1	350	2.531×10^{13}	3.543	0.1521	0.1716
L2	290	3.829×10^{13}	4.276	0.1612	0.1774
L3	190	8.864×10^{13}	6.526	0.3126	0.3795
L4	333	2.523×10^{13}	3.724	0.2921	0.3387

the values of λ_0 and S_0 are obtained. The energy of the oscillator is given by $\varepsilon_0 = hc/e\lambda_0$ (c is the speed of light, h is Plank's constant, and e is the electronic charge). The fitted values of λ_0, S_0 and ε_0 of the LBTN-x thin films are shown in Table 2. One can see from Fig. 3 that the single oscillator dispersion relation fits very well to the experimental data. It was reported that S_0 is independent of the band gap, but depends strongly on the packing density of the material [17]. Therefore, the low value of S_0 obtained here is due to the lower packing density of the films. S_0 increases with the content of La^{3+} except in L4 sample, which means that the densities of L1, L2 and L3 samples increase with the La^{3+} content. The fabricating conditions of the thin films are the same, but the thicknesses of them are different. The thickness of L1, L2, and L3 samples decreases with the La^{3+} content (Table 1). It means that the densities of L1, L2, and L3 samples increase with the La^{3+} content, which is in agreement with the foregoing result.

The Z-scan results without an aperture for the LBTN-x thin films are shown in Figs. 4 and 5. It is obvious from Figs. 4 and 5 that the open-aperture curves comprise normalized transmittance valley, indicating the presence of nonlinear absorption in the film. There are two kinds of nonlinear absorption: multi-photon absorption and free carrier absorption. Because the width of incident laser pulse (100 fs) is much smaller than the recombination time of free carriers in the films (nanosecond or longer), the free carrier absorption effect is negligible. Thus, the nonlinear optical absorption in LBTN-x thin films is attributed to two-photon absorption (2PA) and three-photon absorption (3PA) [18]. Since the bandgap in LBTN-x (3.269–3.525 eV) is larger than the excitation energy of the laser ($2h\nu$ = 3.1 eV), 2PA can not be attributed to a direct transition process. However, 2PA can occur at 800 nm in LBTN-x thin films from strong laser pulse with intermediate levels in the forbidden gap induced by impurities [19].

Utilizing the open apeture Z-scan theory for multiphoton absorption the nonlinear absorption coefficient β can be deduced from the normalized transmittance T for open aperture by Eq. (2) [20,21]:

$$T = \frac{1}{\left[1+(n-1)\beta L_{\text{eff}}(I_0/(1+z/z_0)^2)^{n-1}\right]^{1/n-1}} \quad (2)$$

where $L_{\text{eff}} = \{1-\exp[(n-1)\alpha L]\}/[(n-1)\alpha]$ is the effective film thickness, L is the film thickness, α is the linear absorption coefficient, I_0 is the laser intensity at the focal point, and $z_0 = 2\pi\omega_0^2/\lambda$ is the Rayleigh range of the beam. n is the number of absorbed photons (n = 2 for 2PA; n = 3 for 3PA). Figs. 4 and 5 show the Z-scan results without an aperture for the LBTN-x thin films fitted for 2PA and 3PA, respectively. The nonlinear absorption coefficients β of these thin films are shown in Table 2. Because silica substrate shows very weak nonlinear optical property, the large nonlinear absorption observed here is from the LBTN-x films. The magnitudes of β increase with La^{3+} content of LBTN-x thin films except L4 sample. The magnitude of β depends on impurity band [19]. The total effective intermediate-level density increases with the La^{3+} content of LBTN-x. This is exactly the reason why the two-photon absorption effect enhances when the La^{3+} content of LBTN-x thin films except L4 sample.

The nonlinear absorption coefficient of $SrBi_2Nb_2O_9$, $Bi_{3.25}La_{0.75}Ti_3O_{12}$, $Bi_{3.75}Nd_{0.25}Ti_3O_{12}$, and $Bi_2Nd_2Ti_3O_{12}$ thin films are 1.1×10^{-7}, -6.76×10^{-8}, 5.24×10^{-7}, and 3.1×10^{-7} m/W, respectively [4,5,22,23]. The high nonlinear absorption of LBTN-x film compares favorably with the nonlinearities of good nonlinear optical materials. This means that the new LBTN-x film is promising for applications in nonlinear optical devices. Especially, this thin film may be useful in space vehicles because of its relatively high Curie point (T_c > 900 °C).

As stated above, the linear and nonlinear optical properties of L4 sample are different from those of other samples. According to

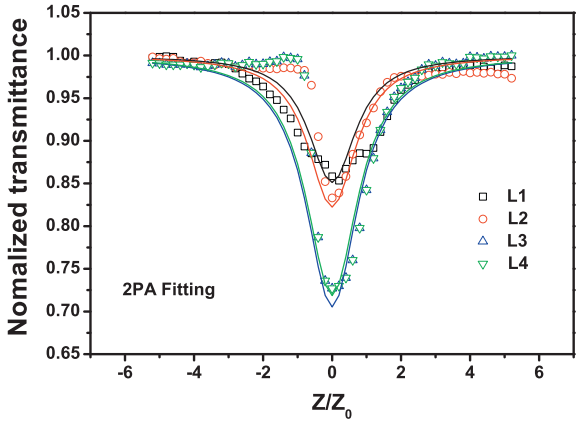

Fig. 4. Open-aperture Z-scan data of LBTN-x thin films measured at 800 nm using 100 fs pulse. The symbols are the measured data and the solid lines are the theoretical fittings for 2PA.

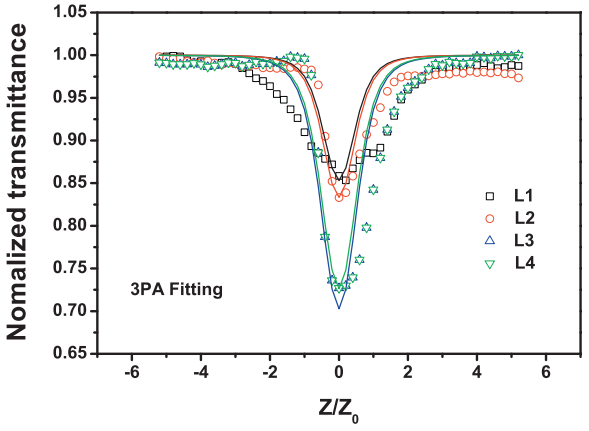

Fig. 5. Open-aperture Z-scan data of LBTN-x thin films measured at 800 nm using 100 fs pulse. The symbols are the measured data and the solid lines are the theoretical fittings for 3PA.

previous studies [9], La^{3+} ions in LBTN-x begin to partly substitute the Bi^{3+} in $(Bi_2O_2)^{2+}$ layers when La^{3+} content $x \geq 25\%$. In L4 sample, $x = 35\%$, the substitution content of Bi^{3+} in $(Bi_2O_2)^{2+}$ layers is high enough to aggravate the orthorhombic distortion of the octahedra, leading to remarkable changes of linear and nonlinear properties of L4 sample compared to other samples. Hence, $x = 25\%$ is the optimal La^{3+} content for LBTN-x to obtain the largest nonlinear absorption coefficient.

4. Conclusion

LBTN-x thin films with layered perovskite structure were prepared on fused silica substrates by the pulsed laser deposition method. The linear optical constants were determined from the transmittance spectra using the envelope method. With increasing La^{3+} content, the refractive index of LBTN-x thin film decreases but the bandgap of the thin film increases. The dispersion in the refractive indexes are fitted by the Sellmeier dispersion relation and described by an electronic oscillator model. Average oscillator strength increases with the content of La^{3+} except L4 sample, in which the La^{3+} content exceeded the critical value. The nonlinear optical properties are obtained using a Z-scan technique at a wavelength of 800 nm with a 100 fs duration laser. The magnitude of β depends on the population of the impurity band. Our results showed that when $x \leq 25\%$, the nonlinear absorption coefficient of LBTN-x increases with the La^{3+} content. For the case of L4 sample, $x = 35\%$, the substituted content of Bi^{3+} in $(Bi_2O_2)^{2+}$ layers is high enough to aggravate the orthorhombic distortion of the octahedra, resulting a remarkable change in linear and nonlinear optical properties. Therefore, $x = 25\%$ is the optimal La^{3+} doping content for LBTN-x to obtain the largest nonlinear absorption coefficient.

Acknowledgement

This work was supported by the National Nature Science Foundation of China (Grant No. 10704021).

References

[1] K.D. Preston, G.H. Haertling, Appl. Phys. Lett. 60 (1992) 2831–2833.
[2] G.H. Jin, B. Nemet, Y.L. Lu, C. Hsu, M.C. Golomb, F.L. Wang, H. Jiang, J. Zhao, Appl. Phys. Lett. 74 (1999) 3116–3118.
[3] B. Yang, Y.P. Wang, F. Wang, Y.F. Chen, S.N. Zhu, Z.G. Liu, W.W. Cao, Appl. Phys. A 81 (2005) 183–186.
[4] K. Chen, H. Gu, J. Zou, W. Li, H. Yi, Mater. Lett. 61 (2007) 3701–3704.
[5] F.W. Shi, X.J. Meng, G.S. Wang, J.L. Sun, T. Lin, J.H. Ma, Y.W. Li, J.H. Chu, Thin Solid Films 496 (2006) 333–335.
[6] B. Yang, H. Chen, M. Zhang, F. Wang, K. Cheah, W. Cao, Appl. Phys. A 96 (2009) 1017–1021.
[7] M. Zhang, H. Chen, B. Yang, W. Cao, Appl. Phys. A 97 (2009) 741–744.
[8] M. Zhang, B. Yang, H. Chen, W. Cao, Opt. Mater. 32 (2009) 406–409.
[9] Z.Y. Zhou, X.L. Dong, H.X. Yan, Scripta Mater. 55 (2006) 791–794.
[10] M. Osada, M. Tada, M. Kakihana, T. Watanabe, H. Funakubo, Jpn. J. Appl. Phys. 40 (2001) 5572–5575.
[11] D.W. Lee, K.W. Seo, S. Cho, S.R. Park, C. Kim, J. Appl. Phys. 99 (2006) 034101.
[12] J. Zhu, X.B. Chen, Z.P. Zhang, J.C. Shen, Acta Mater. 53 (2005) 3155–3162.
[13] J.C. Manifacier, J. Gasiot, J.P. Fillard, J. Phys. E 9 (1976) 1002–1004.
[14] R. Swanepoel, J. Phys. E: Sci. Instrum. 16 (1983) 1214–1222.
[15] A.N. Pikhtin, A.D. Yas'Kov, Sov. Phys. Semicond. 15 (1981) 81.
[16] M. Didomenico, S.H. Wemple, J. Appl. Phys. 40 (1969) 720–734.
[17] R. Thomas, D.C. Dube, Jpn. J. Appl. Phys. 39 (2000) 1771–1775.
[18] K. Venkata Saravanan, K.C. James Raju, M. Ghanashyam Krishna, P.T. Surya, S. Venugopal Rao, Appl. Phys. Lett. 96 (2010) 232905.
[19] Y. Deng, Y.L. Du, M.S. Zhang, J.H. Han, Z. Yin, Solid State Commun. 135 (2005) 221–225.
[20] M. Sheik-bahae, A.A. Said, T.H. Wei, D.J. Hagan, E.W. Van Stryland, IEEE J. Quantum Electron. 26 (1990) 760–769.
[21] R. Sai Santosh Kumar, S. Venugopal Rao, L. Giribabu, D. Narayana Rao, Chem. Phys. Lett. 447 (2007) 274–278.
[22] Y.H. Wang, B. Gu, G.D. Xu, Y.Y. Zhu, Appl. Phys. Lett. 84 (2004) 1686–1688.
[23] B. Gu, Y.H. Wang, X.C. Peng, J.P. Ding, J.L. He, H.T. Wang, Appl. Phys. Lett. 85 (2004) 3687–3689.